

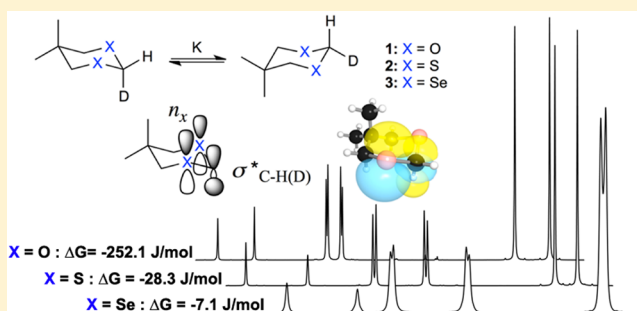
Probing Hyperconjugation Experimentally with the Conformational Deuterium Isotope Effect

Kyle T. Greenway, Anthony G. Bischoff, and B. Mario Pinto*

Department of Chemistry, Simon Fraser University, Burnaby, BC, V5A 1S6, Canada

S Supporting Information

ABSTRACT: Hyperconjugation underlies many chemical phenomena of fundamental and practical importance. Owing to a great deal of interest in the anomeric effect, anomeric-like hyperconjugative effects have been thoroughly investigated in oxygen-containing systems. However, such interactions in the second- and third-row chalcogens are less well-understood and have generated some controversy. Here, we show that the conformational deuterium isotope effect, in combination with Saunders' isotopic perturbation method, permits sensitive and direct experimental probing of the conformational equilibria in dioxane, dithiane, and diselenane analogues by variable-temperature, dynamic NMR spectroscopy. We find that the magnitude of the conformational deuterium isotope effect is 252.1, 28.3, and 7.1 J/mol ($\pm 10\%$) for the oxygen, sulfur, and selenium analogues, respectively. These results reveal the periodic trend for hyperconjugation in the chalcogens, which reflect a decreasing $n_x \rightarrow \sigma_{C-H(D)}$ interaction throughout the period, as supported by IR spectroscopy and in agreement with DFT calculations and a natural bond order analysis.



INTRODUCTION

Structural and conformational phenomena in organic molecules test theoretical frameworks and underpin many questions of chemical stability and reactivity. Frontier molecular orbital (FMO) theory has been largely successful in attributing these phenomena, such as the anomeric effect,^{1,2} to a limited set of critical molecular orbital interactions, including hyperconjugative interactions.³ The concept of hyperconjugation was originally introduced to explain the effects of alkyl substituents on electronic properties of unsaturated compounds in terms of σ - π orbital interactions.^{4,5} It was later extended to discuss various conformational, structural, and reactivity effects in terms of interactions between sigma-bonding orbitals σ or nonbonding (lone pair) orbitals n and sigma-antibonding orbitals σ^* ,⁶ such as the gauche effect,^{7,8} Saytzeff's rule,⁹ and the anomeric effect.¹⁰⁻¹²

Experimental evaluation is complicated by the difficulty of isolating hyperconjugation from other contributing factors, often resulting in controversy.^{13,14} Here we show both experimentally and computationally that the conformational deuterium isotope effect (CDIE) can serve as a minimal perturbation to directly probe the balance of hyperconjugative interactions in the acetal unit of a series of 2-deuterio-5,5-dimethyl-1,3-diheterocyclohexanes ($X = O, S, Se$, Figure 1).

By incorporating a single deuterium at C2 in such cyclic systems, which undergo rapid ring inversion between otherwise degenerate conformations, the resultant difference in free energy ΔG° can be attributed entirely to the competition between deuterium and hydrogen for axial and equatorial

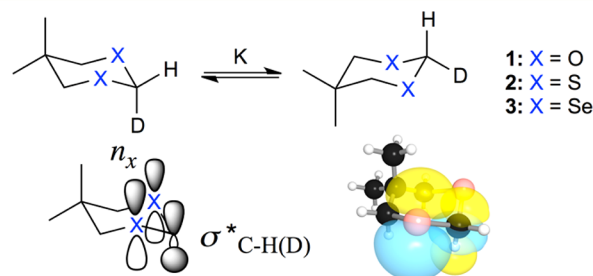


Figure 1. Compounds of interest and one key hyperconjugative interaction. Compounds are 2-deuterio-5,5-dimethyl-1,3-dioxane (1), 2-deuterio-5,5-dimethyl-1,3-dithiane (2), and 2-deuterio-5,5-dimethyl-1,3-diselenane (3). Depicted orbitals are the n_x orbitals present on both chalcogens and the $\sigma^*_{C-H(D)}$, in a simple representation (left) and as calculated by the NBO method (right).

positions. Within the Born–Oppenheimer approximation, hydrogen and deuterium are electronically identical. Therefore, the major determinant of this equilibrium is molecular vibration, in which the energy of the molecule is best minimized when deuterium occupies the stronger bond owing to its lower zero-point energy. Since hyperconjugation lengthens and weakens bonds in which antibonding orbital occupancy is increased or in which bonding orbital occupancy is decreased,⁶ a single deuterium atom at the anomeric position of these systems can translate the balance of the hyper-

Received: August 22, 2012

Published: October 1, 2012

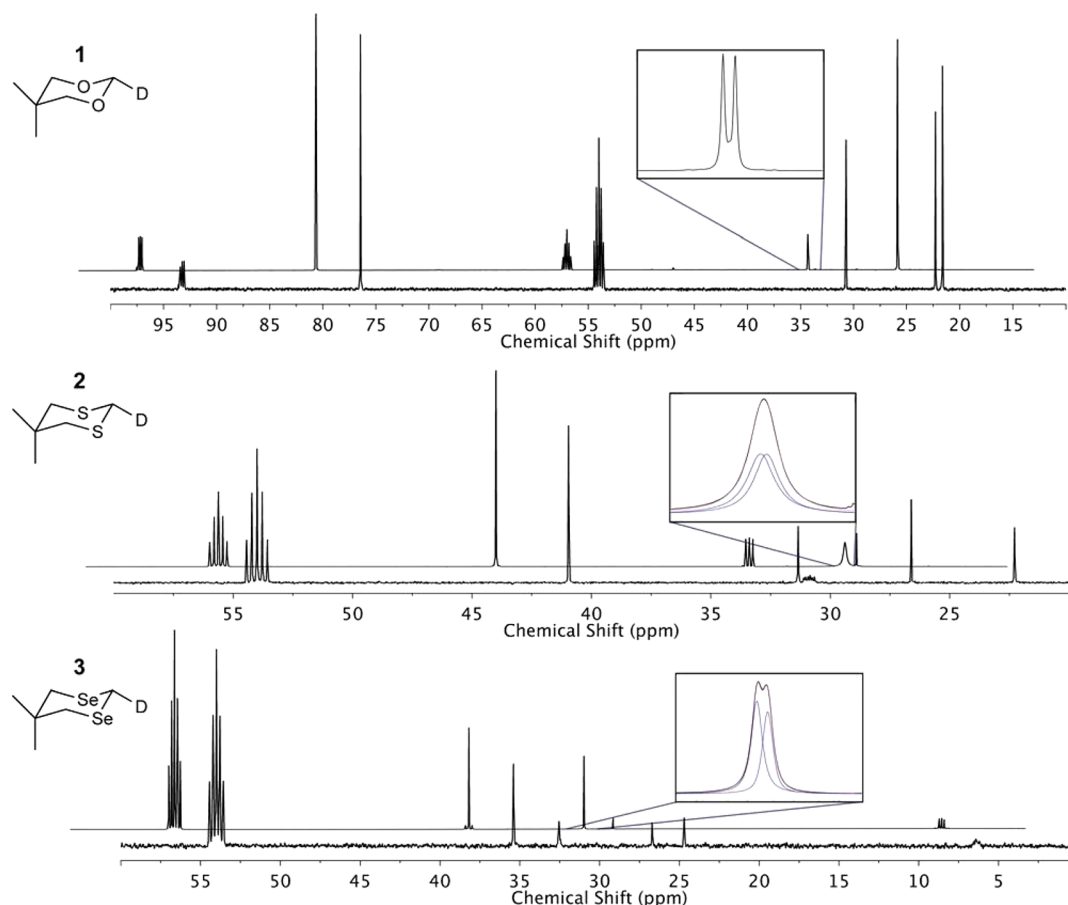


Figure 2. ¹³C room temperature spectra of compounds 1, 2, and 3, in dichloromethane-*d*₂ at 298 K. Inset shows separated signals for methyl groups at room temperature due to the conformational deuterium isotope effect.

conjugative interactions present into the ΔG° of the equilibrium. ΔG° can then be determined using low-temperature nuclear magnetic resonance (NMR) via the isotopic perturbation method of Saunders¹⁵ or, alternatively, by direct integration. Here, we report the values of ΔG° for 5,5-dimethyl-2-deuterio-1,3-dioxane (1), -dithiane (2), and -diselenane (3) using both methods, permitting evaluation of the balance of axial versus equatorial hyperconjugative interactions in these systems.

There is little dispute that hyperconjugation is partly responsible for the anomeric effect with first-row elements (e.g., O), though the exact magnitude of this contribution remains disputed.¹⁶ The dominant interaction is from the p-type lone pair on oxygen n_O to the adjacent axial antibonding σ^* orbital, although several interactions affecting equatorial and axial σ^* orbitals contribute, and it is their balance that is most relevant.^{7,11} Experimental support for the dominance of the axial effects over the equatorial effects includes the longer C-substituent axial bonds relative to C-substituent equatorial bonds,¹⁷ larger $^1J_{C-H}$ coupling constants for the stronger equatorial bonds (Perlin effect),^{18,19} and IR C–H(D) stretching frequencies (Bohlmann bands) that further suggest a weaker axial bond.^{20,21}

In the case of the heavier congener, sulfur, the picture is less clear. Numerous studies on conformational preferences in 2-heterosubstituted thiaheterocycles have demonstrated an anomeric effect,²² although some evidence in the parent heterocycles has led investigators to conclude that hyperconjugation plays little or no role,¹⁹ in contrast to the situation

for oxygen. Specifically, early computational work employing the 6-31G* basis set suggested that the anomeric-like equatorial C–H bond was longer than the axial bond in 1,3-dithiane.²¹ Experimental results with 1,3-dithiane further showed that the $^1J_{C-H}$ coupling constants were reversed in magnitude from those of 1,3-dioxane,²³ ΔG° for the equilibrium of 2 in Figure 1 was reported to be essentially zero;²⁴ IR stretching frequencies for axial and equatorial C2–D bonds were reported to be identical,²⁴ and it was concluded that no CDIE existed.²⁴ However, more recent analyses at higher levels of computation with a variety of methods and with higher-level basis sets have found that the axial bond is in fact longer than the equatorial bond.^{11,25} These differences in axial and equatorial bond lengths and non-equivalent hyperconjugative interactions should result in distinct axial and equatorial IR stretching frequencies and a CDIE (by way of comparison, for the oxygen analogue 1, stretching frequencies differed by 141 cm^{-1} and ΔG° was reported to be 205 J/mol).²⁶

It is now also clear that coupling constants are not straightforward measures of bond strengths since longer and weaker C–H bonds can exhibit larger $^1J_{C-H}$ coupling constants (dubbed the “reverse Perlin effect”) as in dioxane, dithiane, and oxathiane.¹⁰ Detailed natural bond order (NBO) analysis has further shown that sulfur exhibits many of the same hyperconjugative interactions that contribute to the anomeric effect in oxygen, albeit at a somewhat reduced level,¹¹ and $\sigma_{C-H(D)} \rightarrow \sigma^*_{S-C}$ interactions are not dominant as previously postulated in our earlier work.^{18,21}

In the case of systems containing selenium, several studies have demonstrated anomeric effects in selenium coronands²⁷ and diselenanes,^{28,29} and NBO analysis suggests that hyperconjugative interactions similar to sulfur exist.⁶ It is not known whether a CDIE or Bohlmann-type bands are present.

In this work, we have re-evaluated the CDIE and IR spectra for systems containing oxygen (**1**) and sulfur (**2**) and extended the studies to the diselenane (**3**). We confirm that the CDIE is an effective probe of hyperconjugation and provide corrected data for the dithiane system (**2**), which confirms the presence of a CDIE. The collective data reveal a consistent periodic trend for anomeric-like hyperconjugation in the chalcogens, which reflects a $n_x \rightarrow \sigma^*_{C-H(D)}$ interaction that decreases in the order $X = O > S > Se$, as supported by DFT calculations and a natural bond order analysis.

RESULTS AND DISCUSSION

The ¹³C NMR spectra at low temperature and at 298 K for **1–3** (Figure 2) exhibit separated signals due to the CDIE. These separations permitted the determination of ΔG° values, using Saunders isotopic perturbation method,¹⁵ which are listed in Table 1 along with theoretical results for compounds **1–3**. ΔG°

Table 1. Experimental and Computed Values of ΔG°

	Δ (Hz) ^a	ω (Hz) ^b	ΔG° (J/mol) ^c	computed ΔG° (J/mol) ^d
1	116.25	5.91	252.1	299.3
2	1367.52	7.82	28.3	36.8
3	1186.35	1.70	7.1	13.1

^a Δ was measured under conditions of slow exchange at 180 K for **1** and **2** and 156 K for **3** from the 125 MHz ¹³C NMR spectra; value corrected to 150 MHz ¹³C for comparisons. ^b ω was measured under conditions of fast exchange at room temperature in the 150 MHz ¹³C NMR spectra. ^c ΔG° was determined experimentally via eq 2 and the standard relationship $\Delta G^\circ = -RT \ln K$ for $T = 298$ K, with an estimated error of 10%. ^dResults of DFT calculations.

is largest for the dioxane **1**, reduced for the dithiane **2**, and reduced even further for the diselenane **3**, with all systems exhibiting a preference for an equatorial deuterium atom. This preference was successfully established by assignment—utilizing the W effect,^{30,31} T_1 measurements, and predicted NMR spectra,³² all in agreement (see Supporting Information)—and subsequent integration of the H2 signals in the low-temperature ¹H NMR spectra.

Our result of 252 J/mol for the dioxane **1** is similar to the previously reported value of 205 J/mol. However, our result for the dithiane **2** of 28 J/mol differs considerably from the previous report of 0 J/mol. In both cases, we believe our result to be of greater precision due to our use of ¹³C chemical shifts, rather than ¹H chemical shifts, with Saunders' isotopic perturbation method because of the greater spectral dispersion offered by ¹³C spectra. This is significant given that, except for the dioxane **1**, no conformationally separated signals are visible in the ¹H spectra (Supporting Information Figures S2, S4, and S6). For the diselenane **3**, our results suggest a further reduction of ΔG° to 7 J/mol, which marks the lowest measurement of a ΔG° by NMR spectroscopy to our knowledge. These results (Table 1) suggest that the hyperconjugative interactions in dioxane **1** that lengthen the axial C2–H(D) bond are significantly greater than those lengthening the equatorial C2–H(D) bond. Moving down the period, the balance is shifted toward lengthening the equatorial C–H

bond—either due to increasing strength of equatorial interactions, decreasing strength of axial interactions, or both—but parity is not reached.

The results for C–D stretching frequencies, measured by infrared spectroscopy, offer further insight into hyperconjugation. As Table 2 shows, the axial C–D stretching frequency for

Table 2. IR C2–D Stretching Frequencies and Computed Bond Lengths

		exptl IR frequency (cm ⁻¹)	computed IR frequency (cm ⁻¹) ^a	computed bond length (Å) ^a
1	axial	2089	2086	1.1036
	equatorial	2230	2238	1.0864
2	axial	2153	2182	1.0903
	equatorial	2196	2224	1.0874
3	axial	2185	2213	1.0865
	equatorial	2202	2233	1.0860

^aResults of DFT calculations at the B3LYP 6-311G++(3df,3pd) level, with a scaling factor of 0.9673.³³

dioxane **1** is 141 cm⁻¹ less than the equatorial C–D stretching frequency. This suggests a longer (and weaker) bond, as would be expected from dominant axial interactions. In dithiane **2**, however, the axial C–D stretching frequency has increased by 64 cm⁻¹ while the equatorial C–D stretch has decreased by 34 cm⁻¹, narrowing the gap to 43 cm⁻¹. This is consistent with the reduced ΔG° CDIE value being due to both an increase in the equatorial hyperconjugative interactions and a decrease in the axial hyperconjugative interactions. In diselenane **3**, the gap between C–D stretching frequencies is further narrowed to just 17 cm⁻¹, due to a further increase in the C–D axial stretching frequency. The last result corresponds well with the CDIE results, in which the equilibrium constant is only slightly above unity, owing to weaker axial hyperconjugative interactions. In all cases, computed IR stretching frequencies agree well with experimental values (Table 2), although the discrepancy from the previous report of equal axial and equatorial C–D IR stretching frequencies bears addressing. As is evident in our experimental spectra (Supporting Information Figures S8–S10) and in our computed IR intensities (Supporting Information Table S5), the intensities of these stretches are quite low. Further, they are far lower for the dithiane **2** (and the diselenane **3**) than they are for the dioxane **1**. Indeed, the intensity of the C–D_{equatorial} stretch for the dithiane **2** is calculated to be only 4% of that for the dioxane **1** and 2% of the C–D_{axial} stretch intensity for **1**. We therefore suggest that the second IR stretch peak for the dithiane **2** was missed by the previous study due to its surprisingly low intensity.²⁴

Finally, our NBO analysis suggests that these observed trends are consistent with a decreasing $n_x \rightarrow \sigma^*_{C-H}$ interaction in the order $X = O > S > Se$, as summarized in Table 3. The magnitude of the hyperconjugation effect can be evaluated within the framework of standard second-order perturbation theory.³ It is directly proportional to the square of the Fock matrix element F_{ij} (or to the square of orbital overlap S_{ij}) between interacting orbitals i and j and is inversely proportional to the energy gap $\epsilon_j - \epsilon_i$ between these orbitals, as in eq 1.

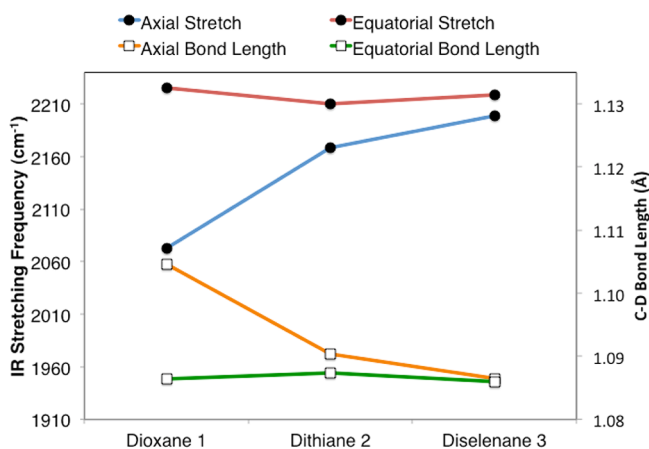
$$\Delta E^2 = \frac{2F_{ij}^2}{\epsilon_j - \epsilon_i} \propto \frac{S_{ij}^2}{\epsilon_j - \epsilon_i} \quad (1)$$

Table 3. Calculated Chalcogen–carbon Bond Lengths and Results of the NBO Analysis

system	X–C2 bond length (Å)	X–C4 bond length (Å)	deletion energy (kJ/mol)	F_{ij} (au) ^a	$\epsilon_i - \epsilon_j$ (au) ^b
1	1.4030	1.4240	23.9	0.054	0.64
2	1.8150	1.8235	17.9	0.046	0.62
3	1.9609	1.9761	13.8	0.041	0.64

^aOff-diagonal Fock matrix elements, corresponding to the orbital resonance integral. ^bDifference in orbital energies.

More accurately, this energy can be assessed using NBO deletion analysis by setting $F_{ij} = 0$ and re-diagonalization of the Fock matrix,³⁴ although some have questioned the NBO framework's validity.³⁵ Our NBO results indicate that the axial $n_x \rightarrow \sigma_{C-H(D)}$ interaction decreases down the period, much like the experimental trends, suggesting that a decreasing anomeric-like interaction contributes to the observed trend. Of the two factors that contribute to the strength of this interaction,⁶ namely, the overlap and the energy difference of the interacting orbitals, orbital overlap is the major factor, as determined from examination of the relevant Fock matrix elements. Orbital overlap is reduced by approximately 15% from dioxane **1** to dithiane **2** and a further 10% to diselenane **3**, corresponding to a decrease in the energy of the hyperconjugative interactions of 6 and 4 kJ/mol, respectively. The decrease in orbital overlap is due to the lengthening of carbon–chalcogen bonds moving down the period (Table 3), which distorts the ring significantly for compounds **2** and **3**. More thorough NBO analyses in first- and second-row systems that more closely examine the balance of the multiple interactions presented have been performed elsewhere,¹¹ and factors such as other vibrational modes and rehybridization may contribute to CDIE magnitudes and the qualitative agreement between experimental values and NBO results. However, we note that the experimental trend is well-described by the key $n_x \rightarrow \sigma_{C-H}$ interaction. This conclusion is supported by the results in Figure 3, which demonstrate that the equatorial C2–H(D) bond remains roughly constant throughout compounds **1**–**3** while the axial bond length changes significantly.

**Figure 3.** Comparison of calculated axial and equatorial C–D bond lengths with observed IR stretching frequencies.

CONCLUSIONS

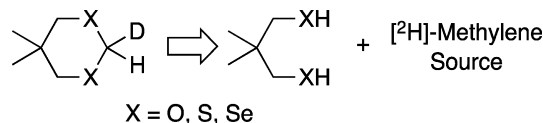
We have shown that the CDIE in combination with IR spectroscopic studies of monodeuterated dioxane **1**, dithiane **2**, and diselenane **3** analogues reveals a simple trend that is reflective of a decreasing anomeric-like hyperconjugation in the top three chalcogens. Sulfur exhibits a CDIE that is reduced by roughly an order of magnitude from oxygen, while the interaction is reduced by nearly 75% further for selenium. NBO analysis suggests that a source of this decrease is a reduction in the anomeric-like $n_x \rightarrow \sigma_{C-H(D)}$ interaction due to the lengthened carbon–chalcogen bond, which decreases the orbital overlap. These results suggest that hyperconjugative interactions affecting axial C–H(D) bonds are greater than those affecting equatorial C–H(D) bonds in second- and third-row systems, similar to the first-row systems. Finally, we confirm that modern theory and experiment are in agreement with respect to the importance of hyperconjugative interactions in this series of chalcogens.

EXPERIMENTAL SECTION

General. Dioxane and its congeners are widely employed model systems for studying hyperconjugation and the anomeric effect.^{6,7,11,17–19,21,22,24,26,28,29} The choice of the specific analogues utilized in the present study is based on several considerations. The employment of a single deuterium at the anomeric C2 position is explained above. The use of two chalcogens in the systems increases the magnitude of the hyperconjugative effects of interest and symmetrizes the molecule, simplifying analysis. Finally, the inclusion of two methyl groups at the C5 position facilitates accurate measurement of the equilibria using Saunders' isotopic perturbation method.¹⁵

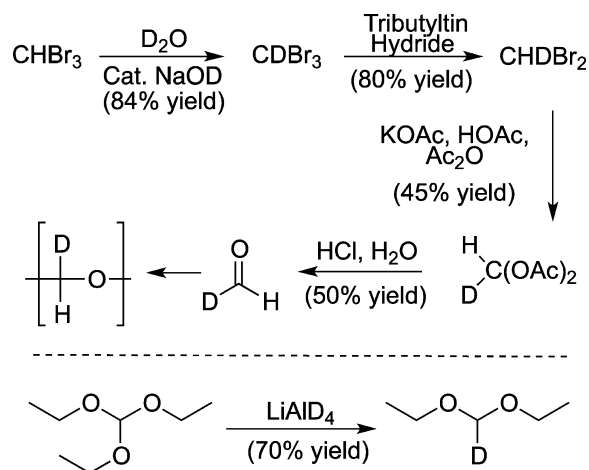
The general retrosynthetic scheme is shown in Scheme 1. The [²H]-methylene unit for the synthesis of the diselenane **3** was derived from

Scheme 1. Retrosynthetic Analysis



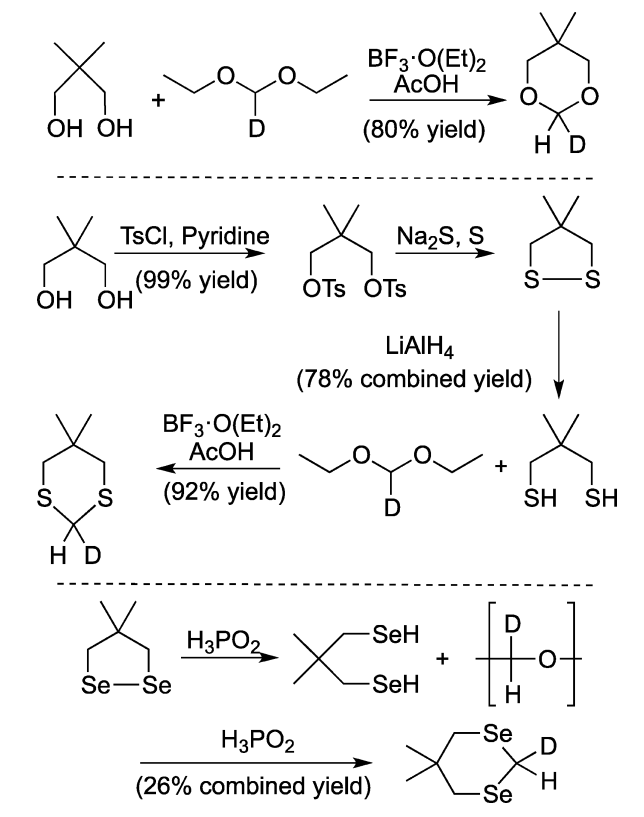
[²H]-paraformaldehyde, while the more convenient [²H]-diethoxymethane (Scheme 2) was employed for the synthesis of dioxane **1** and

Scheme 2. Synthesis of [²H]-Methylene Units: [²H]-Paraformaldehyde (Above) and [²H]-Diethoxymethane (Below)



dithiane **2**. Combination of the [^2H]-methylene unit with the diol equivalents, as shown in Scheme 3, yielded the compounds of interest in satisfactory yields.

Scheme 3. Synthesis of Dioxane 1 (Top), Dithiane 2 (Middle), and Diselenane 3 (Bottom)



5,5-Dimethyl-[$^2\text{H}_1$]-1,3-dioxane (1). The synthesis 5,5-dimethyl-[$^2\text{H}_1$]-1,3-dioxane (**1**) has been described previously.³⁶ Low-temperature ^1H NMR (500 MHz, CD_2Cl_2 , 185 K): δ 4.92 (s, 1H, $\text{H}_{2\text{eq}}$, fwhm = 4.5 Hz), 4.44 (s, 1H, $\text{H}_{2\text{ax}}$, fwhm = 4.2 Hz), 3.51 (d, J = 10.9 Hz, 2H, $\text{H}_{4\text{eq}}/\text{H}_{6\text{eq}}$), 3.32 (d, J = 10.9 Hz, 2H, $\text{H}_{4\text{ax}}/\text{H}_{6\text{ax}}$), 1.08 (s, 6H, Me_{ax}), 0.63 (s, 6H, Me_{eq}). Room-temperature ^1H NMR (500 MHz, CD_2Cl_2 , 185 K): δ 4.72 (s, 2H, H2), 3.46 (s, 4H, H4/H6), 0.94 (d, J = 11.7 Hz, 12H, Me). Low-temperature ^{13}C NMR (125 MHz, CD_2Cl_2 , 185 K): δ 93.26 (1:1:1 t, J = 24.5 Hz, C2), 76.45 (s, C4/C6), 30.72 (s, C5), 22.28 (s, Me_{ax}), 21.63 (s, Me_{eq}). Room-temperature ^{13}C NMR (150 MHz, CD_2Cl_2 , rt) δ 94.18 (1:1:1 triplet, J = 24.9 Hz, C2), 77.64 (s, C4/C6), 31.31 (s, C5), 22.84 (d, J = 5.92 Hz). FTIR (ATR): 2230, 2089.

5,5-Dimethyl-[$^2\text{H}_1$]-1,3-dithiane (2). [^2H]-diethoxymethane was synthesized by known procedures,³⁷ as was the 2,2-dimethyl-1,3-dithiol.³⁸ In a 5 mL flask equipped with a micro stirrer and a condenser, the dithiol (160 mg, 1.17 mmol) was combined with [^2H]-diethoxymethane (150 mg, 1.43 mmol), boron trifluoride etherate (0.18 mL, 1.4 mmol), acetic acid (0.35 mL, 6.1 mmol), and chloroform (3 mL). The solution was refluxed overnight. The product was diluted to 10 mL with dichloromethane and washed alternately with water and 0.1 M NaOH, three times each. The resultant liquid was dried over sodium sulfate and chromatographed on a silica column in 99:1 pentane/ethyl acetate. The isolated product was condensed under rotary evaporation and distilled in a microdistillation apparatus to yield dithiane **2** as a pale yellow oil (160 mg, 92%). Low-temperature ^1H NMR (500 MHz, CD_2Cl_2 , 185 K): δ 3.82 (s, 1H, $\text{H}_{2\text{ax}}$, fwhm = 4.1 Hz), 3.29 (s, 1H, $\text{H}_{2\text{eq}}$, fwhm = 5.7 Hz), 2.71 (d, J = 10.9 Hz, 2H, $\text{H}_{4\text{eq}}/\text{H}_{6\text{eq}}$), 2.27 (d, J = 10.9 Hz, 2H, $\text{H}_{4\text{ax}}/\text{H}_{6\text{ax}}$), 1.15 (s, 6H, Me_{ax}), 0.96 (s, 6H, Me_{eq}). Room-temperature ^1H NMR (600 MHz, CD_2Cl_2 , rt): δ 3.60 (s, 1H, H2), 2.55 (s, 4H, H4/H6), 1.15 (s,

6H, Me). Low-temperature ^{13}C NMR (125 MHz, CD_2Cl_2 , 185 K): δ 40.95 (s, C4/C6), 31.34 (s, Me_{eq}), 30.89 (1:1:1 t, J = 23.5 Hz, C2), 26.61 (s, C5), 22.29 (s, Me_{ax}). Room-temperature ^{13}C NMR (150 MHz, CD_2Cl_2 , rt): δ 42.41 (s, C4/C6), 31.82 (1:1:1 t, J = 22.9 Hz, C2), 27.83 (br s, Me), 27.34 (s, C5). HRMS (EI): m/z calcd for $\text{C}_6\text{H}_{11}\text{DS}_2$ [M] 149.0443, found 149.0469. FTIR (ATR): 2196, 2153.

5,5-Dimethyl-[$^2\text{H}_2$]-1,3-diselenane (3). 4,4-Dimethyl-1,2-disele-nolane²⁸ (150 mg, 0.63 mmol) was added to hypophosphorous acid (7 mL) in a 50 mL round-bottom flask. A condenser fitted with a N_2 bubbler was attached to a 25 mL two-necked flask containing [^2H]-paraformaldehyde (78 mg, 1.25 mmol), prepared by known procedures³ and several drops of both phosphoric acid and hypophosphorous acid. The two-necked flask served as the receiver on a distill-head which was purged with nitrogen and quickly attached to the 50 mL flask. The diselenide mixture was heated with stirring over 30 min, after which a 2,2-dimethyl-1,3-propanediselenol/water mixture was distilled over at 90 °C and collected in the receiver. Under a blast of nitrogen, the two-necked receiver was removed and stoppered. (Note: the diselenol is extremely sensitive to oxidation by air back to the diselenide.) The mixture was refluxed for 24 h, cooled, then extracted with ether (2 \times 10 mL). The combined ether extracts were washed with water (10 mL) and concentrated, leaving a dark-red liquid. The product was chromatographed on silica (hexane/ethyl acetate, 100:1) and distilled (bulb-to-bulb under vacuum at 80 °C) to yield the product as an oil (40 mg, 26%). Low-temperature ^1H NMR (500 MHz, 95:5, $\text{CCl}_2\text{F}_2/\text{CD}_2\text{Cl}_2$, 158 K): δ 3.81 (s, 1H, $\text{H}_{2\text{ax}}$, fwhm = 10.9 Hz, T_1 = 706 ms), 3.25 (s, 1H, $\text{H}_{2\text{eq}}$, fwhm = 12.7 Hz, T_1 = 732 ms), 2.98 (d, J = 11.5 Hz, 4H, $\text{H}_{4\text{ax}}/\text{H}_{6\text{ax}}$), 2.37 (d, J = 11.5 Hz, 4H, $\text{H}_{4\text{eq}}/\text{H}_{6\text{eq}}$), 1.31 (s, 6H, Me_{ax}), 1.27 (s, 6H, Me_{eq}). Room-temperature ^1H NMR (600 MHz, CD_2Cl_2 , rt): δ 3.54 (1:1:1 triplet, 1H, H2), 2.65 (s, 4H, H2/H4), 1.24 (s, 6H, Me). Low-temperature ^{13}C NMR (125 MHz, 95:5, $\text{CCl}_2\text{F}_2/\text{CD}_2\text{Cl}_2$, 168 K): δ 35.39 (s, C4/C6), 32.54 (s, Me_{eq}), 26.70 (s, C5), 24.70 (s, Me_{ax}), 6.34 (1:1:1 t, J = 22.2 Hz, C2). Room-temperature ^{13}C NMR (CD_2Cl_2 , 150 MHz, rt): δ 35.52 (s, C4/C6), 28.28 (d, J = 1.7 Hz, Me), 26.46 (s, C5), 5.82 (1:1:1 t, J = 23.5 Hz, C2). HRMS (EI): m/z calcd for $\text{C}_6\text{H}_{12}\text{DSe}_2$ [$M - \text{H}$]⁺ 245.9405, found 245.9424. FTIR (ATR): 2202, 2185.

Spectroscopic Analysis. NMR room-temperature spectra were recorded on a 600 MHz spectrometer equipped with a QNP cryoprobe with deuterated dichloromethane as the solvent. Low-temperature spectra were recorded on a 500 MHz spectrometer in deuterated dichloromethane for **1** and **2** and with $\text{CCl}_2\text{F}_2/\text{CD}_2\text{Cl}_2$ (90:10) for **3**. Axial and equatorial methyl ^{13}C signals were measured at several temperatures and chemical shifts linearly extrapolated to room temperature for use in eq 2. Curve fitting, as implemented in the software program MestReNova 6.2.1, was used to accurately determine the separation of signals. Assignment of peaks is discussed in Supporting Information. Theoretical NMR shifts, used as further support of the spectral assignments, were computed with the gauge-independent atomic orbital (GIAO) method³² (Supporting Information Tables S1 and S3) as implemented in Gaussian 09. Infrared spectra were recorded at room temperature on an attenuated total reflectance Fourier transform IR spectrometer (ATR-FTIR) and were assigned based on comparison to previous work and by computed IR stretching frequencies.

The standard method of determining equilibrium constants is direct integration of the NMR spectra at sufficiently low temperatures at which conformational exchange is slow on the NMR time scale, yielding the equilibrium populations at that temperature. However, the CDIE are small in magnitude, as hydrogen/deuterium are "weak" acceptors or donors of the hyperconjugative interactions of interest.¹⁰ Therefore, only small variations in bond lengths are being probed and a more sensitive measurement technique is required.

The Saunders isotopic perturbation method is perfectly suited to this task. With this technique, the symmetrical methyl groups, which do not affect the equilibrium or the chemical shifts at C2, facilitate measurement of ΔG° as follows. Given a non-unity equilibrium, one of the methyl groups at C5 will spend slightly more time in the axial position and the other slightly more time in the equatorial position. Thus, the ^1H and ^{13}C NMR spectra will exhibit separated signals

rather than an exchange-averaged signal even at temperatures at which exchange is fast on the NMR time scale. The magnitude of the separation will depend on two factors: the chemical shift difference between the environments and the equilibrium constant. In order to obtain the latter, the former must be measured at several temperatures sufficiently low for exchange to be slow on the NMR time scale and extrapolated to room temperature.

The equilibrium constant can be obtained quantitatively from a simple expression as a function of the observed separation ω and the observed separation in the low-temperature signals Δ (derivation in Supporting Information):

$$K = (\Delta - \omega) / (\Delta + \omega) \quad (2)$$

Computational. Calculations were performed with the Gaussian 09 software package with B3LYP functional and the 6-311G+(3df,3pd) basis set.^{39,40} Justification for this choice is presented in the Supporting Information, section 4. Optimized structures were identified as minima with zero imaginary vibrational frequencies, and the coordinates and energies of each are given in the Supporting Information. Free energies were calculated at 298.15 K, including zero-point energy and thermal contributions. Isotope substitution was performed for axial and equatorial deuterium orientations by setting the appropriate hydrogen's mass to 2 amu for additional frequency calculations. Reported frequencies were scaled by a factor of 0.9673,³⁵ which is optimized for B3LYP at this basis set. The NBO analysis was performed with the NBO 5.0 package, run externally from output of G09.³⁴

■ ASSOCIATED CONTENT

● Supporting Information

Derivation of eq 2, description of spectral assignments, ¹³C and ¹H room-temperature and low-temperature NMR spectra, IR spectra, computational details for basis selection choice and predicted NMR shifts, computed IR intensities, computed geometries, and energies. This material is available free of charge via the Internet at <http://pubs.acs.org>.

■ AUTHOR INFORMATION

Corresponding Author

*E-mail: bpinto@sfu.ca.

Notes

The authors declare no competing financial interest.

■ ACKNOWLEDGMENTS

The authors thank A. Lewis for technical assistance, N. Weinberg for helpful discussions, and the Natural Sciences and Engineering Research Council of Canada for financial support in the form of a Canada Graduate Scholarship (to K.T.G.) and a grant (to B.M.P.). This article is dedicated to the memories of three inspiring individuals, F.A.L. Anet, B.D. Johnston, and S. Wolfe.

■ REFERENCES

- (1) Edward, J. T. *Chem. Ind.* **1955**, 36, 1102–1104.
- (2) Lemieux, R. U.; Chu, N. J. In *Abstracts of Papers*; 133rd National Meeting of the American Chemical Society; San Francisco, CA, 1958; Vol. 33, p 31N.
- (3) Albright, T. A.; Burdett, J. K.; Whangbo, M. *Orbital Interactions in Chemistry*; 1st ed.; Wiley: Chichester, UK, 1985.
- (4) Mulliken, R. S. *J. Chem. Phys.* **1939**, 7, 339–352.
- (5) Mulliken, R. S.; Rieke, C. A.; Brown, W. G. *J. Am. Chem. Soc.* **1941**, 63, 41–56.
- (6) Alabugin, I. V.; Gilmore, K. M.; Peterson, P. W. *WIREs Comput. Mol. Sci.* **2011**, 1, 109–141.
- (7) Whangbo, M.-H.; Wolfe, S. *Isr. J. Chem.* **1980**, 20, 36–42.

- (8) Goodman, L.; Gu, H.; Pophristic, V. *J. Phys. Chem. A* **2005**, 109, 1223–1229.
- (9) Braida, B.; Prana, V.; Hiberty, P. C. *Angew. Chem., Int. Ed.* **2009**, 48, 5724–5728.
- (10) Alabugin, I. V.; Zeidan, T. A. *J. Am. Chem. Soc.* **2002**, 124, 3175–3185.
- (11) Alabugin, I. V. *J. Org. Chem.* **2000**, 65, 3910–3919.
- (12) Pinto, B. M.; Schlegel, H. B.; Wolfe, S. *Can. J. Chem.* **1987**, 65, 1658–1662.
- (13) Cocinero, E. J.; Carcabal, P.; Vaden, T. D.; Simons, J. P.; Davis, B. G. *Nature* **2011**, 469, 76–79.
- (14) Wang, C.; Ying, F.; Wu, W.; Mo, Y. *J. Am. Chem. Soc.* **2011**, 133, 13731–13736.
- (15) Saunders, M.; Jaffe, M. H.; Vogel, P. *J. Am. Chem. Soc.* **1971**, 93, 2558–2559.
- (16) Mo, Y. *Nat. Chem.* **2010**, 2, 666–671.
- (17) Romers, C.; Altona, C.; Buys, H. R.; Havinga, E. In *Topics in Stereochemistry*; Eliel, E. L., Allinger, N. L., Eds.; John Wiley & Sons, Inc.: Hoboken, NJ; Vol. 4, pp 39–97.
- (18) Wolfe, S.; Pinto, B. M.; Varma, V.; Leung, R. Y. N. *Can. J. Chem.* **1990**, 68, 1051–1062.
- (19) Juaristi, E.; Cuevas, G. *Acc. Chem. Res.* **2007**, 40, 961–970.
- (20) Bohlmann, F. *Angew. Chem.* **1957**, 69, 641–642.
- (21) Wolfe, S.; Kim, C.-K. *Can. J. Chem.* **1991**, 69, 1408–1412.
- (22) Juaristi, E.; Cuevas, G. *Tetrahedron* **1992**, 48, 5019–5087.
- (23) Bailey, W. F.; Rivera, A. D.; Rossi, K. *Tetrahedron Lett.* **1988**, 29, 5621–5624.
- (24) Anet, F. A. L.; Kopelevich, M. *J. Chem. Soc., Chem. Commun.* **1987**, 595–598.
- (25) Juaristi, E.; Cuevas, G.; Vela, A. *J. Am. Chem. Soc.* **1994**, 116, 5796–5804.
- (26) Anet, F. A. L.; Kopelevich, M. *J. Am. Chem. Soc.* **1986**, 108, 2109–2110.
- (27) Batchelor, R. J.; Einstein, F. W. B.; Gay, I. D.; Gu, J. H.; Johnston, B. D.; Pinto, B. M. *J. Am. Chem. Soc.* **1989**, 111, 6582–6591.
- (28) Pinto, B. M.; Johnston, B. D.; Nagelkerke, N. *Heterocycles* **1989**, 28, 389–403.
- (29) Mikołajczyk, M.; Mikina, M.; Graczyk, P.; Wieczorek, M. W.; Bujacz, G. *Tetrahedron Lett.* **1991**, 32, 4189–4192.
- (30) Pinto, B. M.; Sandoval-Ramirez, J.; Dev Sharma, R. *Tetrahedron Lett.* **1985**, 26, 5235–5238.
- (31) Pinto, B. M.; Johnston, B. D.; Sandoval-Ramirez, J.; Sharma, R. D. *J. Org. Chem.* **1988**, 53, 3766–3771.
- (32) Cheeseman, J. R.; Trucks, G. W.; Keith, T. A.; Frisch, M. J. *J. Chem. Phys.* **1996**, 104, 5497–5509.
- (33) Merrick, J. P.; Moran, D.; Radom, L. *J. Phys. Chem. A* **2007**, 111, 11683–11700.
- (34) Reed, A. E.; Weinhold, F. *J. Chem. Phys.* **1985**, 83, 1736–1740.
- (35) Bickelhaupt, F. M.; Baerends, E. J. *Angew. Chem., Int. Ed.* **2003**, 42, 4183–4188.
- (36) Ouzounian, J. G.; Anet, F. A. L. *J. Labelled Compd. Radiopharm.* **1986**, 23, 401–404.
- (37) Hanley, J. A.; Forsyth, D. A. *J. Labelled Compd. Radiopharm.* **1990**, 28, 307–310.
- (38) Eliel, E. L.; Smith, V. S.; Hutchins, R. O. *J. Org. Chem.* **1975**, 40, 524–526.
- (39) Becke, A. D. *Phys. Rev. A* **1988**, 38, 3098–3100.
- (40) Lee, C.; Yang, W.; Parr, R. G. *Phys. Rev. B* **1988**, 37, 785–789.